

## IDENTIFICATION OF A B32 METASTABLE PRECIPITATE IN THE FE-BE SYSTEM

M. K. Miller, M. G. Burke and S. S. Brenner  
U. S. Steel Research Laboratory, Monroeville, PA 15146

W. A. Soffa  
University of Pittsburgh, Pittsburgh, PA 15261

K. B. Alexander and D. E. Laughlin  
Carnegie-Mellon University, Pittsburgh, PA 15213

(Received December 27, 1983)

#### Introduction

The decomposition of iron-rich supersaturated iron-beryllium solid solutions has been the subject of many investigations; however, many aspects of the decomposition reactions are still unresolved (1, 2, 3, 4). The equilibrium phase diagram indicates that the  $\alpha$  solid solution decomposes into a hexagonal (C14)  $\text{FeBe}_2$  phase and  $\alpha$ -ferrite (5). A low temperature metastable miscibility gap exists which intersects a higher order order-disorder transition (Figure 1). In the region below both the miscibility gap and the order-disorder transition, the ferrite first orders (B2) and then decomposes by spinodal decomposition to form a triaxially aligned microstructure consisting of ferrite and an ordered B2 beryllium-enriched phase (1, 6, 7). Davies and Richman (3), on the basis of x-ray diffraction results, have reported that there is also a  $\text{DO}_3$  ( $\text{Fe}_3\text{Be}$ ) ordering which occurs in the ordered (B2) matrix. At aging temperatures within the miscibility gap, the aligned  $\alpha'' + \text{B2}$  microstructure has been reported to be replaced by a metastable precipitate. In general, the metastable precipitate forms in a cooperative manner with the ferrite resulting in a two-phase morphology similar to cellular (or discontinuous) precipitation (1). In this case, however, the reaction front is not a high angle grain boundary and there is no matrix re-orientation across the reaction front. At aging temperatures above the miscibility gap, the first decomposition product is the metastable precipitate, and it forms in the same morphology described above. Yagisawa and Yoshida (8, 9) have suggested that the metastable precipitate has the C15 structure ( $\text{Cu}_2\text{Mg}$ ) with  $a = 6.2\text{\AA}$ ; Higgins (1) *et al.* report it to be "face-centered tetragonal" with  $a = 5.76\text{\AA}$ ,  $c/a = .89$ , and Heubner (10) proposes a tetragonal structure with  $a = 2.789$  and  $c/a = .97$ . The equilibrium phase forms at all temperatures upon prolonged aging.

In this paper, the identification of the metastable precipitate is presented. The combined techniques of atom probe field-ion microscopy and transmission electron microscopy have been used to provide both microstructural and microchemical information to identify conclusively the metastable phase.

#### Experimental Procedure

The material used in this investigation was an Fe-25 at% Be alloy. The alloy was solution-treated at  $1100^\circ\text{C}$  prior to isothermal aging in the temperature range  $265^\circ$  to  $515^\circ\text{C}$ . All atom probe microchemical analyses were carried out with a specimen temperature of 30 K in the presence of a trace of neon imaging gas. The unrestricted mass range of the atom probe allows direct quantitative analysis of beryllium. The beryllium was found to evaporate predominantly as  $\text{Be}^{2+}$  with a small amount of  $\text{Be}^+$  at this temperature. The field-ion micrographs were recorded using neon as an imaging gas either at 30 K for maximum atomic resolution or between approximately 80 - 100 K for maximum contrast between the phases.

Electron microscopy of thin foil specimens was performed on a JEOL 200CX Temscan operating at 200kV. In order to assist in the phase identification, computer generated electron diffraction patterns were constructed using the positions of the atoms in the unit cell and the specific unit cell geometry to calculate the appropriate structure factors.

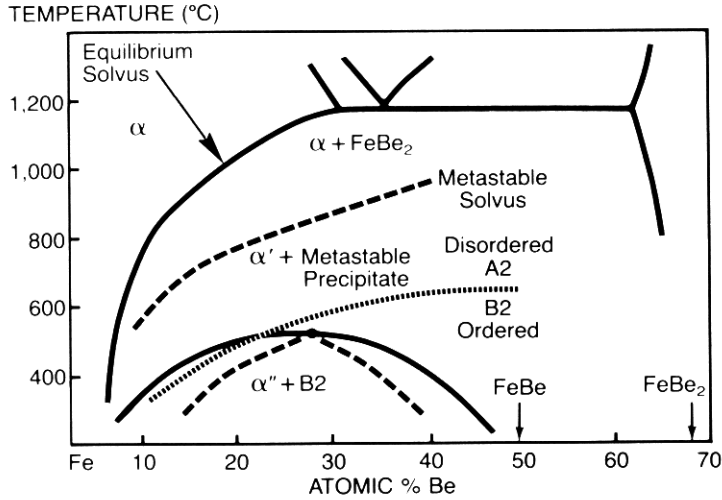


Figure 1: Schematic phase diagram of the Fe-Be system.

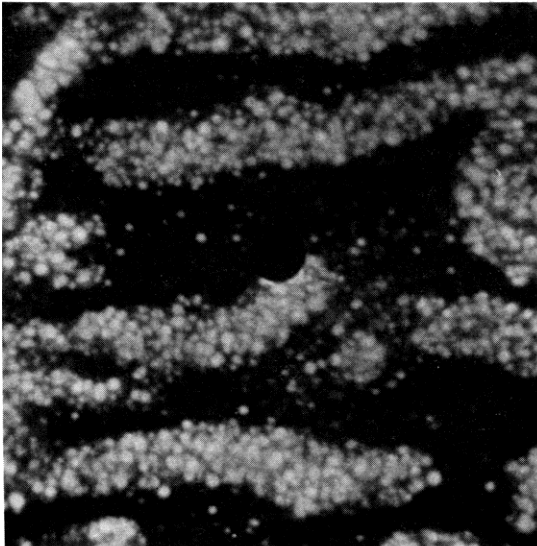


Figure 2a: Field-ion micrograph of the metastable precipitate in a specimen aged 2 hours at 450°C.

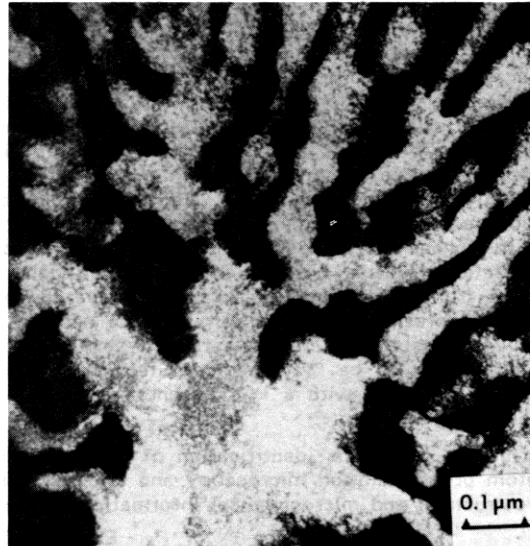


Figure 2b: Dark-field TEM micrograph of the metastable precipitate imaged using {111} B32 reflection. Aged 13.5 hours at 514°C.

**Results**

The microstructure formed after aging above the miscibility gap consists of the metastable precipitate in a ferrite ( $\alpha'$ ) matrix as shown in the field-ion micrograph in Figure 2(a). Selected area atom probe analysis revealed that the brightly imaging regions are the metastable precipitate in the darkly imaging ferrite matrix. A dark-field transmission electron micrograph using a metastable precipitate reflection is shown for comparison in Figure 2(b).

At temperatures within the miscibility gap, the metastable precipitate was found to consume the

crystallographically aligned modulated microstructure of ferrite ( $\alpha''$ ) + B2 which formed as a result of prior spinodal decomposition. In the field ion micrographs containing the modulated structure, the darkly imaging phase within this structure was found to be the ordered B2 phase (11).

The composition of the metastable precipitate was determined from atom probe selected area analysis to be  $49.5 \pm 1.1$  at% Be after aging 13.5 hours at  $514^\circ\text{C}$  and  $48.0 \pm 2.2$  at% Be after aging 149 hours at  $350^\circ\text{C}$ . The corresponding compositions of the coexisting ferrite ( $\alpha'$ ) matrix were  $4.5 \pm .9$  and  $3.5 \pm .7$  at% Be respectively.

A high resolution field-ion micrograph of a specimen aged 13.5 hours at  $514^\circ\text{C}$  is shown in Figure 3(a). The microstructure consists of a two-phase ferrite ( $\alpha'$ ) and metastable precipitate mixture. In this micrograph, the contrast between the two phases is substantially reduced due to the low specimen temperature (30 K). The entire micrograph can be indexed as single crystal and the prominence of the major poles (through both phases) indicates that both the matrix and the metastable precipitate have crystal structures in which the atoms occupy body-centered cubic sites. The ring-matching apparent in Figure 3(b) demonstrates that atomic registry exists between the metastable phase and the  $\alpha'$  matrix; this evidence together with the crystallographic correspondence in Figure 3(a) indicates a high degree of coherency between the two phases.

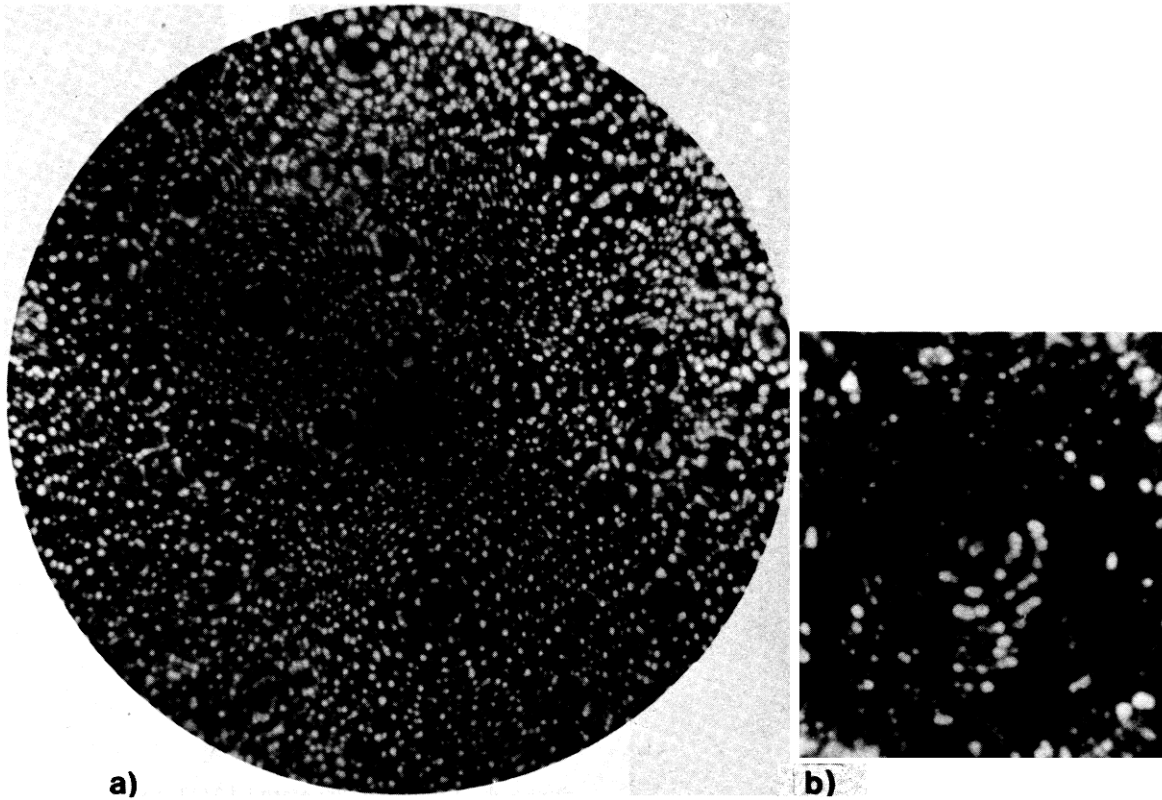


Figure 3a: High resolution field-ion micrograph of the coexisting ferrite and metastable precipitate. Specimen aged 149 hours at  $350^\circ\text{C}$ .

Figure 3b: Field-ion micrograph of a specimen aged 13.5 hours at  $514^\circ\text{C}$  showing ring matching between the ferrite and the metastable precipitate.

### Discussion

The consistent bcc indexing and the coherency deduced from the field-ion micrographs indicates that the metastable precipitate is a derivative of the body-centered cubic crystal structure. This observation excludes the possibility that the phase is the equilibrium hexagonal  $\text{FeBe}_2$  phase. The diffraction pattern obtained from the metastable precipitate, using a  $\langle 011 \rangle$  zone axis, is shown in Figure 4(b). Also shown in Figure 4 are the computer-generated diffraction patterns for various bcc derivative structures. The atomic arrangements on the bcc cell for these structures are shown in Figure 5. The diffraction pattern in Figure 4(b) exhibits systematic absences along the  $\langle 444 \rangle_S$ -type directions<sup>1</sup> identical to those expected for a B32 structure. The B32 structure has the space group  $Fd\bar{3}m$  ( $4_1/d, \bar{3}, 2/m$ ) (5) and can be envisioned as two interpenetrating diamond cubic structures, one containing Fe atoms, and one containing Be atoms. The stacking of the  $\{111\}$ ,  $\{11\bar{3}\}$  and  $\{3\bar{3}1\}$ -type planes in the B32 structure is ABBB...; whereas in the A2 (bcc) structure, the stacking is AAAA.... Thus, the real space periodicity in these directions for the B32 structure is four times that of the A2 structure. This results in all of the fundamental A2  $\langle 222 \rangle_a$ ,  $\langle 226 \rangle_a$  and  $\langle 662 \rangle_a$ -type reciprocal lattice vectors being 'split' into fourths by the B32 superlattice reflections. However, due to the presence of glide planes in the B32 structure, systematic absences of superlattice reflections are obtained whenever the sum of  $(h+k+l)_S/2$  is an odd whole number. Therefore, the  $\{200\}_S$ ,  $\{222\}_S$ ,  $\{226\}_S$  and  $\{662\}_S$ -type reflections will be absent in the B32 diffraction pattern. As a result of

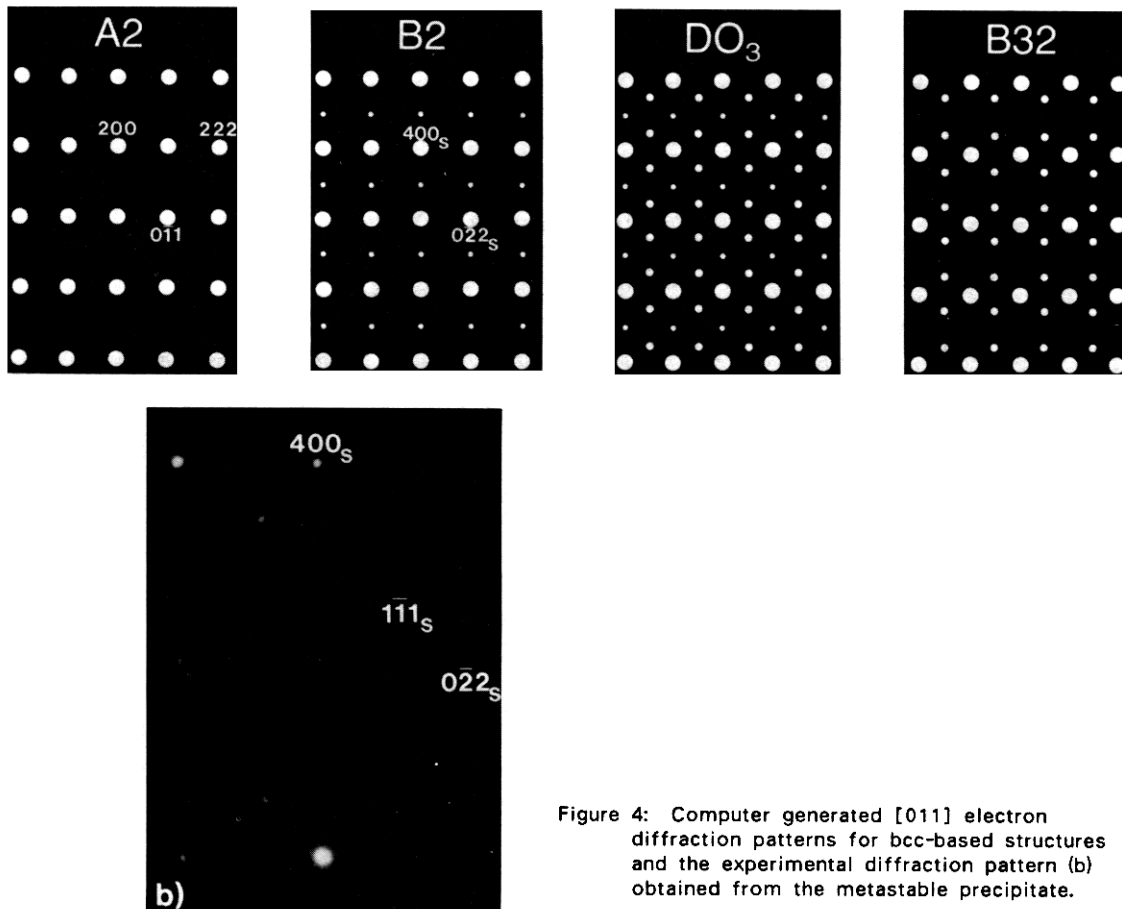


Figure 4: Computer generated [011] electron diffraction patterns for bcc-based structures and the experimental diffraction pattern (b) obtained from the metastable precipitate.

<sup>1</sup>  $\{hkl\}_S$  is the notation with reference to the cell shown in Figure 5. Note that  $\{hkl\}_a$  would be the same reciprocal lattice position as  $\{2h, 2k, 2l\}_S$ .

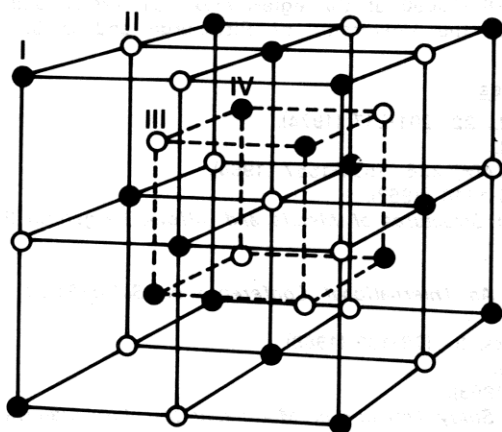


Figure 5: Lattice sites for bcc derivative structures. For B32 (AB) (shown above): sites I and IV are A atoms, sites II and III are B atoms. For B2 (AB): sites I and II are A atoms, III and IV sites are B atoms. For  $DO_3$  ( $A_3B$ ): sites I, II and IV are A atoms, sites III are B atoms.

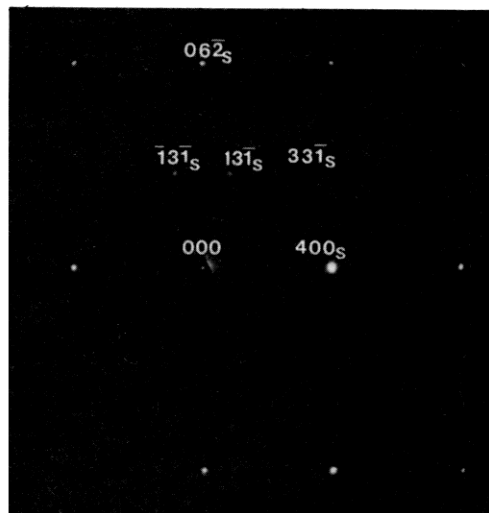


Figure 6:  $\langle 013 \rangle$  selected area electron diffraction pattern showing  $\{113\}_s$  and  $\{331\}_s$  superlattice reflections obtained from the metastable precipitate.

these considerations, the B32 superlattice reflections will be at the one-quarter and three-quarters  $\{222\}_a$ ,  $\{226\}_a$  and  $\{662\}_a$  reciprocal lattice positions only; the one-half positions being absent due to the presence of the glide planes. A diffraction pattern from the  $\langle 013 \rangle$  zone axis is shown in Figure 6. The systematic absences of the  $\{226\}_s$  and  $\{662\}_s$  superlattice reflections further confirm the identification of the metastable phase as B32. In addition, the  $\langle 100 \rangle$  zone axis diffraction pattern contains no superlattice reflections at the  $\{200\}_s$  [ $\{100\}_a$ ] position, consistent with a B32 structure. The observed results are not consistent with those obtained by Higgins *et al.*. The C15 ( $Cu_2Mg$ ) structure proposed by Yagisawa and Yoshida possesses the same space group as the B32 structure and would give a very similar diffraction pattern; however, the stoichiometry of the metastable phase is  $\bar{A}B$ , as measured by atom probe microanalysis, not  $AB_2$ . Additionally, the lattice parameter proposed by Yagisawa and Yoshida is inconsistent with the complete coherency observed in the field-on micrographs and electron diffraction patterns. An interesting observation is that the superposition of the superlattice reflections of the B2 and B32 structures would yield a diffraction pattern that would be similar to  $DO_3$ .

#### Relative Stability of Ordered Phases

A recent paper by Ino (6) suggests that in the Fe-Be system, the first nearest neighbor interaction energy is positive, the second negative, and their relative magnitude approximately  $V_2/V_1 = -4/3$ . In this regime the ground state of a bcc alloy will be an  $a'' + B2$  two phase mixture (12, 13). The  $DO_3$  structure is metastable for  $V_2/V_1 < -4/3$  (for  $V_2 < 0$ ,  $V_1 > 0$ ), and the B32 structure is unstable with respect to the original disordered solid solution (14).<sup>2</sup> In  $V_2/V_1$  regimes where the B32 phase is stable and the B2 phase metastable, the magnitudes of the interaction parameters are such as to preclude the occurrence of spinodal decomposition (14). Including the third nearest neighbor contributions in the calculations for the ground state does not stabilize the B32 phase in regimes where the B2 phase and spinodal decomposition can occur. The stability of the ordered phases in Fe-Be based on chemical and magnetic interaction effects will be discussed in another paper.

#### Acknowledgements

The authors would like to kindly thank Dr. A. Guha of Brush-Wellman Corp. for supplying the Fe-Be alloys; and G. Pierini of Carnegie-Mellon University for the use of the diffraction pattern generation program. The research was funded through NSF DMR-81-05090 at Carnegie-Mellon University and NSF DMR-80-22225 University/Industrial Cooperative grant at the University of Pittsburgh and U. S. Steel Research Laboratory.

#### References

1. J. Higgins, R. B. Nicholson and P. Wilkes, *Acta Met.*, **22**, 201-217 (1974).
2. K. Yagisawa, *Phys. Stat. Sol. (a)*, **18**, 589-596 (1973).
3. R. G. Davies and R. H. Richman, *Trans. Met. Soc. AIME*, **236**, 1551-1557 (1964).
4. M. Heimendahl and U. Heubner, *Acta Met.*, **11**, 1115-1116 (1963).
5. W. B. Pearson, *A Handbook of Lattice Spacings and Structures of Metals and Alloys*, Pergamon Press, (1958).
6. H. Ino, *Acta Met.*, **26**, 827-834 (1978).
7. W. A. Soffa and D. E. Laughlin, *Proceedings of An International Conference on Solid-Solid Phase Transformations*, 159-183, (1981).
8. K. Yagisawa and H. Yoshida, *Jap. JI. Appld. Physics*, **8**, 179-190 (1969).
9. K. Yagisawa, *Phys. Stat. Sol. (a)*, **16**, 291-297 (1973).
10. U. Heubner, *Archiv fur das Eisenhutt.*, **7**, 547-554 (1963).
11. W. A. Soffa et al., *Proceedings of NATO Advanced Study Institute of Modulated Structure Materials*, , (1983).
12. M. J. Richards, D.Sc. Dissertation, M.I.T., Cambridge, MA (1971) .
13. S. M. Allen and J. W. Cahn, *Acta Met.*, **20**, 423-433 (1972).
14. K. B. Alexander, L. L. Lee and D. E. Laughlin, Unpublished research Carnegie-Mellon University